Archives of Mechanics • Archiwum Mechaniki Stosowanej • 26, 6, pp. 965–979, Warszawa 1974

Two-dimensional, two-phase flow with phase transition in a de Laval nozzle

M. BRATOS AND M. BURNAT (WARSZAWA)

THE AIM of this paper is to calculate the two-dimensional, non-equilibrium, two-phase flow in a de Laval nozzle and to compare it with the one-dimensional approximation. The following two types of a flow are considered in two nozzles of different shapes: 1) the pure water steam flow with a relative gas expansion rate of an order of magnitude of $\dot{p} \sim 10^5$ 1/sec. 2) the moist air flow with a relative gas expansion rate of an order of magnitude of $\dot{p} \sim 10^3$ 1/sec. Numerical results for the two-dimensional flow are compared with experimental ones. They point to a fact, that a two-dimensional approach changes appreciably the qualitative picture of the diabatic flow compared with one-dimensional one. The two-dimensional results agree better with experimental ones.

Celem pracy jest numeryczne znalezienie rozwiązania dwuwymiarowego, dwufazowego przepływu z nierównowagową przemianą fazową (kondensacją albo krystalizacją) w dyszy de Lavala i porównania go z rozwiązaniem dla jednowymiarowej aproksymacji. Rozpatrywane są dwa rodzaje przepływów w dyszach o różnych kształtach: 1) przepływ czystej pary wodnej charakteryzujący się względną szybkością ekspansji rzędu: $\dot{p} \sim 10^5$ 1/sec, 2) przepływ wilgotnego powietrza charakteryzujący się względną szybkością ekspansji rzędu $\dot{p} \sim 10^3$ 1/sec. Rezultaty numeryczne dla dwuwymiarowego przepływu są porównane z wynikami eksperymentalnymi (dla wilgotnego powietrza) oraz z rezultatami numerycznymi dla przepływu jednowymiarowego. Wskazują one na fakt silnego wpływu uwzględnienia dwuwymiarowości na jakościowy obraz diabatycznego przepływu. Rozwiązanie dwuwymiarowego przepływu daje lepszą zgodność z doświadczeniem niż rozwiązanie przepływu jednowymiarowego.

В работе строится численным путем двумерное двуфазное течение с неравновесным фазовым переходом в сопле Лаваля. Результаты сравниваются с одномерным приближением и с экспериментом.

Notation

(y, s) coordinates system, s—coordinate along streamline,

$\mathbf{V} = [u, v]$ velocity vector of the flow,

ϱ_m, ϱ, p, T density of two-phase mixture, gas density, pressure (air+water vapour), gas temperature, respectively,

ϱ_c density of condensed (crystallized) phase,

μ mass fraction of the new phase (liquid or solid phase),

p_v, p_i the partial pressure of water vapour and air, respectively,

T_D drop temperature (for "surface-averaged" drop),

p_D (hypothetical) ambient pressure which would be necessary to keep the drop in equilibrium, both drop and vapour having temperature T_D,

$p_\infty(T)$ flat-film saturation pressure corresponding to the temperature T,

$\mathscr{R}$ universal gas constant,

ω_0 specific humidity,

φ_0 relative humidity,

k Boltzmann's constant,

μ_v, μ_i molecular weights for water vapour and air,

μ_{iv} molecular weight (for gas mixture),
γ_v, γ_i ratios of specific heats (water vapour, air),

$$R = R_v = \frac{\mathscr{R}}{\mu_v}, \quad R_i = \frac{\mathscr{R}}{\mu_i},$$

m, V_c mass of one water molecule, volume of one water molecule,
h_m specific enthalpy for a two-phase mixture,
h_{vc} heat of phase transition (specific),
c_{p_v} specific heat of the water vapour,
c_{p_0} specific heat of the gas (air+water vapour — stagnation point),
c specific heat of condensed (crystallized) phase,
δ correction factor,
r drop radius,
r^* critical drop radius,
σ surface tension (for a drop)
I nucleation rate (per unit volume, per unit time),
$\bar{r}$ "surface-averaged" radius,
$\frac{dr}{dt}$ drop growth rate,
$\Delta(d, s)$ the surface of the cross-section of a stream tube,
ξ condensation coefficient,
α, α_i thermal accommodation coefficients for water vapour and air,
D, D_1, D_2 variables introduced to reduce the integro-differential equation of the condensation rate to four first-order differential equations,
A^* vertex distance.

1. Model assumptions

THE AIM of this paper is to calculate the two-dimensional, steady, non-equilibrium, two-phase flow in a de Laval nozzle and to compare it with the one-dimensional approximation.

The following assumptions are introduced:

1. The mass fraction of the condensed, incompressible phase is small.

2. The gas in the flow is inviscid, non-heat-conducting and may be treated as a perfect gas.

3. In the considered model, the bulk heat of condensation (specific, latent) is the difference between the specific enthalpies of the liquid and gas phases (h_c and h_v, respectively) in spite of the fact, that temperatures of the liquid and gas phases are different.

4. The liquid (solid) phase appears in the form of spherical drops or spherical pieces of ice. The drops do not deform during the flow and they do not interact with each other. There is no velocity slip at the surface of the drops.

5. In the considered case of the moist air flow with supply parameters in the stagnation conditions: $p_0 = 753.1$ mm Hg, $T_0 = 290.8$ °K, $\varphi_0 = 0.58$, the temperature decreases down to about 40 °C below a temperature of the triple point. From earlier experimental work of other authors it follows that below -40 °C there appears a non-crystalline form of ice which we regard here as ice spheres [1, 2, 3].

6. A semi-empirical model of nucleation is assumed, which is a modification of the classical Frenkel, Zeldovich nucleation rate [6].

This modification is confined to the introduction of the coefficient of proportionality obtained by comparing numerical and laboratory experiments. In the case of moist air flow in the de Laval nozzle, there was the possibility to compare the numerical results with experimental data. For the flow of pure water vapour we use the classical Frenkel, Zeldovich nucleation rate.

7. It is not completely clear whether the appearance of the crystallized phase is connected with the sublimation of ice crystals directly from the vapour (gas) phase, or with crystallization of the supercooled water drops which are created during the phase transition. The model of sublimation of clusters having the structure of ice with density $\varrho_c = 1.15$ g/cm^3 is assumed [7].

8. The values of the mean molecular free path in the gas are appreciably higher than the sizes of water drops or ice clusters, hence the Hertz-Knudsen's model of exchange of mass and energy between two phases can be applied.

9. Hill's model giving a possibility to introduce the idea of the "surface-averaged" drop radius is adopted [4, 5]. All drops of different sizes in a certain cross-section of stream tube have the same growth rate, which is equal to that of an "average" drop.

To describe the meaning of a "surface-averaged" droplet radius, let us consider a streamline and a stream tube in the neighbourhood of it (Fig. 1). A symbol s denotes a coordinate along this streamline. A condensation process starts at $s = 0$, d denotes a cross-section of a stream tube at the point $s = 0$. All drops, which are convected by a gas

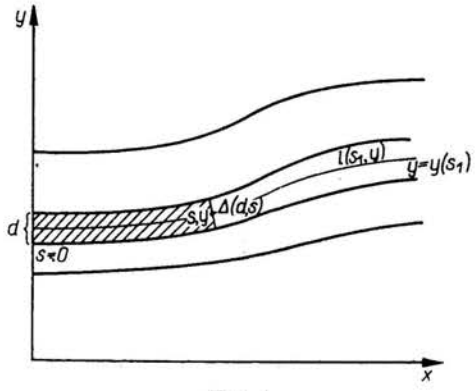

FIG. 1.

through the stream tube cross-section at the point s were created in the region (shadowed in Fig. 1), where $0 \leqslant s_1 \leqslant s$.

Therefore the following definition of a "surface-averaged" droplet radius can be introduced:

$$(1.1)\quad 4\pi\bar{r}^2 = \frac{D^*(d,s)}{D_2^*(d,s)} = \frac{4\pi \int_0^s I(y(s_1),s_1)\Delta(d,s_1)\left(r_0 + \int_{s_1}^s \frac{dr}{dt}\frac{ds_2}{\sqrt{u^2+v^2}}\right)^2 ds_1}{\int_0^s I(y(s_1),s_1)\Delta(d,s_1)ds_1},$$

where $D^*(d, s)$ denotes the cross-sections flux of all drops through the infinitesimal stream tube cross-section $\Delta(d, s)$ and $D_2^*(d, s)$ is the all drops flux through this cross-section $\Delta(d, s)$.

10. According to ALTY, MACKAY and HILL [4, 8] the value of condensation coefficient ξ is taken equal to $\xi = 0.04$ and the value of the thermal condensation coefficient equal to 1 for pure water vapour. In the case of moist air flow, both thermal accommodation and condensation coefficients are taken $\alpha = \alpha_i = \xi = 1$.

2. Equations

From the point of view of the numerical approach the y, s coordinates system is introduced. Therefore the set of continuity, momentum and energy equations for two-dimensional, steady, diabatic flow is as follows:

$$\operatorname{div}(\varrho_m \mathbf{V}) = 0, \tag{2.1}$$

$$\varrho_m(\mathbf{V}\nabla)\mathbf{V} = -\nabla p, \tag{2.2}$$

$$\left(h_m + \frac{u^2+v^2}{2}\right)_{,s} = 0, \tag{2.3}$$

where

$$\varrho_m = \frac{\varrho}{1-\mu}. \tag{2.4}$$

On the base of the assumption 3 the energy equation (2.3) is reduced to the equation:

$$\left(c_{p_0}T + \frac{u^2+v^2}{2} - \mu h_{vc}\right)_{,s} = 0. \tag{2.5}$$

The set of the Eqs. (2.1), (2.2), (2.5) is not full equations system for the two-phase mixture flow.

The equation of a state of a perfect gas:

$$p = \varrho R T, \tag{2.6}$$

where

$$R = \frac{\mathscr{R}}{\mu_{iv}} \tag{2.7}$$

and

$$\frac{1-\mu}{\mu_{iv}} = \frac{1-\omega_0}{\mu_i} + \frac{\omega_0-\mu}{\mu_v}, \tag{2.8}$$

must be added as well as an expression for the relative rate of formation of a new phase $\mu_{,s}$ along the nozzle. Therefore a nucleation rate may be introduced:

$$I = \delta\left(\frac{p_v}{kT}\right)^2 V_c \sqrt{\frac{2\sigma}{\pi m}} \exp\left\{\frac{-4\pi\sigma(r^*)^2}{3kT}\right\}, \tag{2.9}$$

where

$$r^* = \frac{2\sigma}{\varrho_c RT \ln(p_v/p_\infty)} \quad \text{and} \quad R = \frac{\mathcal{R}}{\mu_v} \tag{2.10}$$

as well as the mass and energy conservation equations for the growing drop [4]:

$$\frac{dr}{dt} = \frac{\xi}{\varrho_c}\left(\frac{p_v}{\sqrt{2\pi RT}} - \frac{p_D}{\sqrt{2\pi RT_D}}\right), \tag{2.11}$$

$$\frac{dr}{dt}\varrho_c\left(\frac{\gamma_v}{\gamma_v - 1}RT_D - h_{vc}(T_D)\right) = \frac{\xi p_v K_v RT}{\sqrt{2\pi RT}} + \frac{(1-\xi)p_v K_v RT}{\sqrt{2\pi RT}} - \frac{(1-\xi)p_v K_v R[T+\alpha(T_D-T)]}{\sqrt{2\pi RT}} - \frac{\xi p_D K_v RT_D}{\sqrt{2\pi RT_D}} - \frac{p_i \alpha_i K_i R_i (T_D - T)}{\sqrt{2\pi R_i T}}, \tag{2.12}$$

where

$$K_v = \frac{0.5(\gamma_v+1)}{\gamma_v - 1}, \qquad K_i = \frac{0.5(\gamma_i+1)}{\gamma_i - 1} \tag{2.13}$$

and where

$$h_{vc} = h_{vc0} + (c_{p_v} - c)(T - T_0), \tag{2.14}$$

$$p_D = p_\infty(T_D)\exp\left(\frac{2\sigma}{\varrho_c RT_D \bar{r}}\right), \tag{2.15}$$

$$p_\infty(T) = p_\infty(T_0)\left(\frac{T}{T_0}\right)^{\frac{c_{p_v}-c}{R}} \exp\left[\left(\frac{T_0}{T} - 1\right)\left(\frac{c_{p_v}-c}{R}\right) - \frac{h_{vc0}}{R}\left(\frac{1}{T} - \frac{1}{T_0}\right)\right]. \tag{2.16}$$

The rate at which a new phase forms in the flow is deduced from the analysis of the nucleation process in a given fluid volume as well as analysis of all drops, which enter this volume.

Therefore the following set of differential equations describes the relative rate of formation of liquid (solid) phase during the flow:

$$\sqrt{u^2+v^2}\,\mu_{,s} = \frac{\varrho_c}{\varrho_m}\left\{D(s,y)\varrho_m \frac{d\bar{r}}{dt} + \frac{4\pi}{3} r_0^3 I(s,y)\right\}, \tag{2.17}$$

$$\sqrt{u^2+v^2}\,D_{,s} = \frac{4\pi r_0^2 I(s,y)}{\varrho_m} + D_1\left(\frac{d\bar{r}}{dt}\right), \tag{2.18}$$

$$\sqrt{u^2+v^2}\,D_{1,s} = \frac{8\pi r_0 I(s,y)}{\varrho_m} + D_2\left(\frac{d\bar{r}}{dt}\right), \tag{2.19}$$

$$\sqrt{u^2+v^2}\,D_{2,s} = \frac{8\pi I(s,y)}{\varrho_m}, \tag{2.20}$$

where D, D_1, D_2 are variables introduced to reduce the one integrodifferential equation to four simultaneous first-order differential equations.

$D(s,y)$, $D_1(s,y)$, $D_2(s,y)$ are defined as follows: Let us denote by $l(s,y)$ the streamline passing the point (s,y) (Fig. 1). The streamline equation is:

$$y = y(s_1). \tag{2.21}$$

Then

$$D(s, y) = 4\pi \int_0^s \left[\frac{I(y(s_1), s_1)}{\varrho_m \sqrt{u^2+v^2}} \left(r_0 + \int_{s_1}^s \frac{dr}{dt} \frac{ds_2}{\sqrt{u^2+v^2}} \right)^2 \right] ds_1, \tag{2.22}$$

$$D_1(s, y) = 8\pi \int_0^s \frac{I(y(s_1), s_1)}{\varrho_m \sqrt{u^2+v^2}} \left(r_0 + \int_{s_1}^s \frac{dr}{dt} \frac{ds_2}{\sqrt{u^2+v^2}} \right) ds_1, \tag{2.23}$$

$$D_2(s, y) = 8\pi \int_0^s \frac{I(y(s_1), s_1)}{\varrho_m \sqrt{u^2+v^2}} ds_1. \tag{2.24}$$

The initial condition for the mixed problem is formulated in the isentropic part of the supersonic flow and:

$$D_0 = D_{10} = D_{20} = \lim_{s\to 0} D = \lim_{s\to 0} D_1 = \lim_{s\to 0} D_2 = 0. \tag{2.25}$$

The initial condition for the "surface-averaged" drop $\bar{r}$ is deduced from its definition (1.1). Therefore we have:

$$\lim_{s\to 0} \bar{r}(s, y)^2 = \bar{r}(0, y)^2 = r_0^2. \tag{2.26}$$

The initial condition for the drop temperature is obtained from the conservation energy equation for the growing drop (2.12) taking into account the equality:

$$\bar{r} = r_0. \tag{2.26}$$

In the particular case, $r_0 = r^*$, and it implicates $T_D = T$.

3. The numerical method

The determination of a diabatic, supersonic, two-dimensional flow in the Laval nozzle is reduced to solving the mixed problem for the set of eight partial differential equations (2.1), (2.2), (2.5), (2.17)–(2.20).

This problem is formulated as follows:

1. The initial conditions obtained as a solution of a nonwell-posed Cauchy problem, in a certain Laval nozzle cross-section in the supersonic part of the flow are given.

2. The boundary conditions at the wall of a Laval nozzle of given shape must be kinematic and so they give a well-posed mixed problem.

From the numerical point of view, the solution of a mixed problem is reduced to finding the solution of a difference mixed problem by using the modified Lax scheme [9, 10, 11]. The y, s coordinates are introduced in the case of a solving the mixed problem.

The modified Lax scheme introduces the following difference ratios instead of the derivatives (Fig. 2).

$$\frac{\partial f}{\partial y_*} \approx \frac{f(p) - \dfrac{w_1 f(Q_1) + w_2 f(Q_2)}{w_1 + w_2}}{\Delta y_*}, \tag{3.1}$$

$$\frac{\partial f}{\partial x_*} \approx \frac{f(Q_2) - f(Q_1)}{x_*(Q_2) - x_*(Q_1)}, \tag{3.2}$$

where

$$w_1 = \frac{y_*(Q) - y_*(Q_2)}{y_*(Q_1) - y_*(Q_2)}, \tag{3.3}$$

$$w_2 = 1 - w_1. \tag{3.4}$$

In this case

$$y_* = s, \quad x_* = y, \quad \Delta s = \Delta y_* = y_*(P) - y_*(Q). \tag{3.5}$$

If $w_1 = w_2 = 1$ the modified Lax scheme is reduced to Lax scheme.

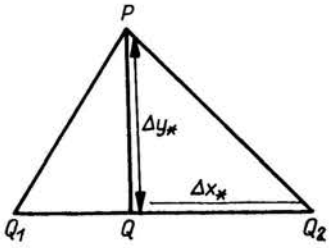

FIG. 2. A modified Lax scheme.

The initial conditions for the mixed problem are found numerically by a solving the transonic, isentropic flow in a plane Laval nozzle. The Cauchy problem for the transonic flow is solved by using the explicit Lax scheme.

The initial conditions for the Cauchy problem are formulated along the symmetry axis of the nozzle as a solution of the one-dimensional isentropic flow in the Laval nozzle with the known geometry.

4. Results

The following two types of flow are considered in two nozzles of different shapes (Fig. 3a, b):

1. The pure water steam flow with a relative gas expansion rate of an order of magnitude of $\dot{p} \sim 10^5$ 1/sec([1]).

2. The moist air flow with a relative gas expansion rate of an order of $\dot{p} \sim 10^3$ 1/sec.

([1]) $\dot{p} = -\dfrac{1}{p}\dfrac{dp}{dt} = -\dfrac{\sqrt{u^2+v^2}}{p}\dfrac{dp}{ds}$

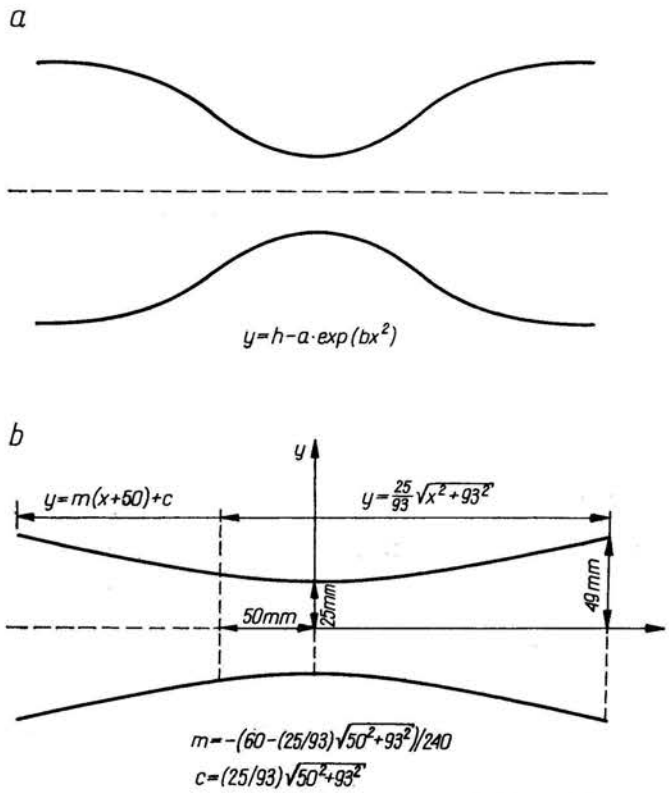

FIG. 3. a) The geometry of the nozzle with water vapour. b) The shape of the nozzle constructed by M. JAESCHKE at the Göttingen Max Planck Institute (moist air).

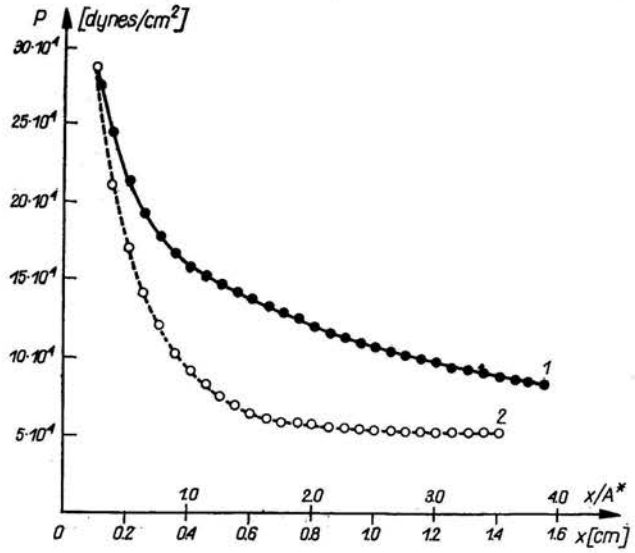

FIG. 4. Static pressure distributions for one- and two-dimensional flows with condensation (axis of the nozzle):

1 — ● — two-dimensional flow with condensation, 2 — — — ○ — — — one-dimensional flow with condensation.

In the case of water steam flow, as a result of a high relative gas expansion rate for both isentropic and diabatic flows, difference appears between solutions of two- and one dimensional flows.

The illustration of this fact can be the pressure (density) distribution of a two-dimensional flow at the axis of symmetry and at the nozzle wall (Fig. 4), where we observe appreciable deviations from the one-dimensional approximation. This deviation is larger than the pressure rise effect connected with phase change, so the influence of a two-dimensional

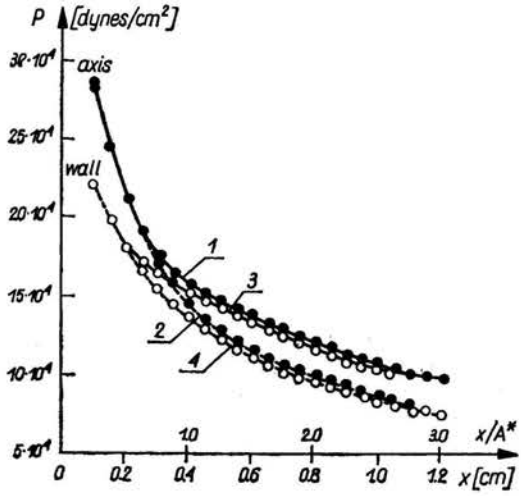

FIG. 5. Static pressure distributions at the nozzle axis and wall for the flows with condensation and without condensation (two-dimensional flow):

1 — ● — the flow with condensation (axis), 2 — — ● — — — the flow without condensation (axis), 4 — — ○ — — the flow without condensation (wall), 3 — ○ — the flow with condensation (wall).

approach screens the condensation phenomenon, (Fig. 5); it also changes the qualitative picture of phase change.

This is also shown in Fig. 6 which presents the temperature distributions along the symmetry axis and the nozzle wall.

In the case of two-dimensional flow we observe a characteristic minimum of the temperature distribution in the region of maximum supercooling and a maximum in the region where equilibrium begins.

These two points define the structure of the condensation "jump". Such a structure is not marked in the case of one-dimensional flow.

In the case of moist air, for the nozzle with a low expansion rate, a small difference between numerical solution of one- and two-dimensional problems would be expected.

Nevertheless, it was shown that even in the case where the one-dimensional solution approximates well the two-dimensional results of the isentropic flow, the two-dimensional treatment introduces a qualitative change in the picture of the flow with a condensation (Fig. 7). This is substantiated by the pressure distribution at the wall and at the axis of symmetry (Figs. 8, 9, 10).

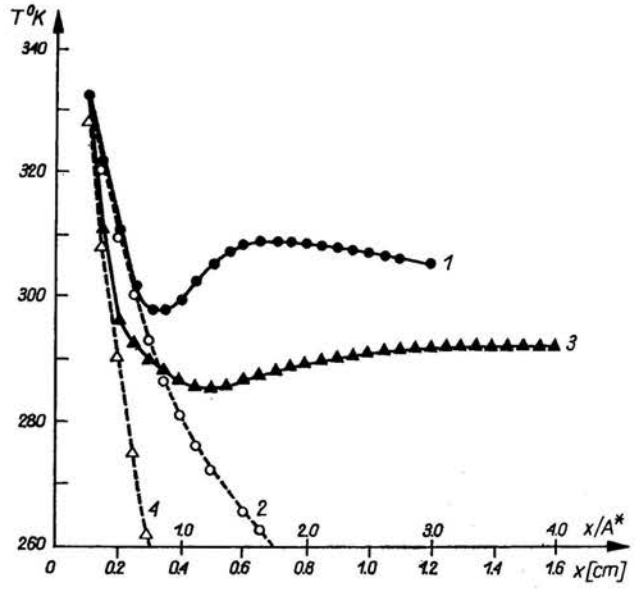

FIG. 6. Temperature distributions for one- and two-dimensional flows with condensation and without condensation (steam, axis of the nozzle):

1 — ● — two-dimensional flow with condensation, 2 — — ○ — — two-dimensional flow without condensation, 3 —▲— one-dimensional flow with condensation, 4 — — △ — — one-dimensional flow without condensation.

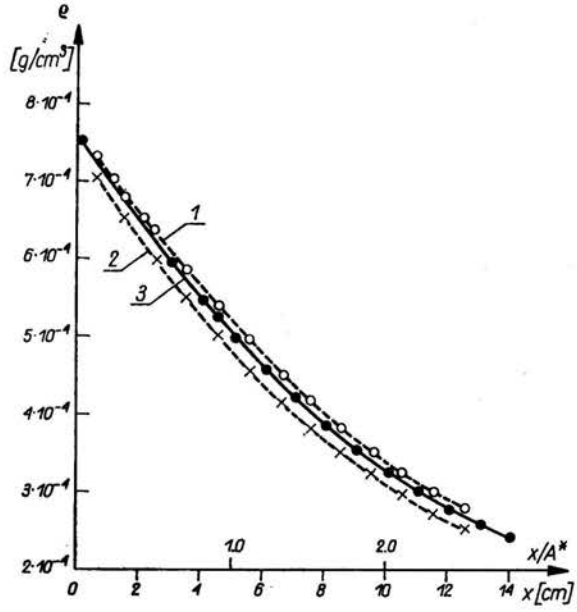

FIG. 7. Gas density distributions (moist air) for one- and two-dimensional isentropic flows:

1 — — ○ — — the axis of the nozzle (two-dimensional flow), 2 — — × — — the wall of the nozzle (two-dimensional flow) 3 — ● —one-dimensional flow.

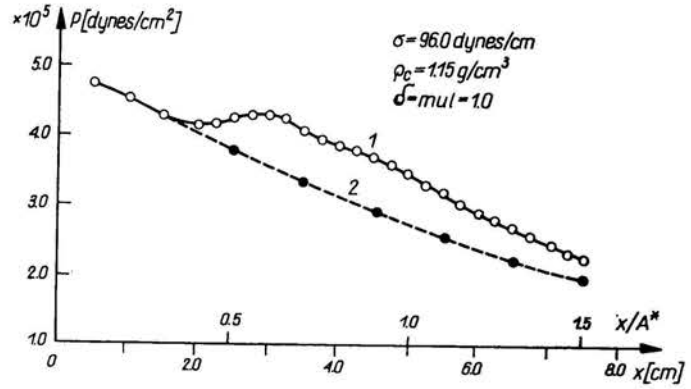

FIG. 8. Static pressure distributions at the nozzle wall for the isentropic flow and for the flow with phase change:
1 —○— diabatic flow, 2 — — ● — — isentropic flow, $\sigma = 96$ dynes/cm, $\varrho_c = 1.15$ g/cm^3, $\delta = 1.0$.

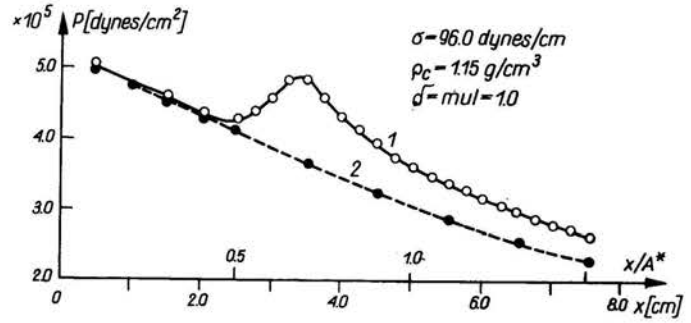

FIG. 9. Static pressure distributions at the nozzle axis for the isentropic flow and for the flow with phase change:
1 —○— diabatic flow, 2 — — ● — — isentropic flow, $\sigma = 96$ dynes/cm, $\varrho_c = 1.15$ g/cm^3, $\delta = 1.0$.

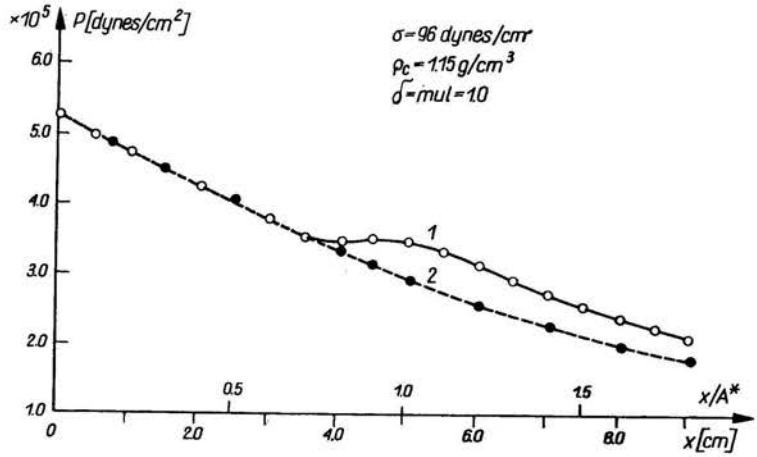

FIG. 10. Static pressure distributions for one-dimensional, diabatic and isentropic flows:
1 —○— diabatic flow, 2 — — ● — — isentropic flow, $\sigma = 96$ dynes/cm, $\varrho_c = 1.15$ g/cm^3, $\delta = 1.0$.

For the nozzle wall as well as for the axis of symmetry, the phase change zone appears in two-dimensional flow at a higher pressure and at a lower Mach number than in the one-dimensional case. The pressure rise in diabatic flow in relation to the isentropic one is larger than in the one-dimensional case. Particularly (Fig. 9) for the pressure distribution at the symmetry axis there appears a characteristic condensation "jump" structure from the point of maximum supercooling to the point of reaching the thermodynamic equilibrium. The structure of the condensation zone has a two-dimensional character, even for a nozzle with a low gas expansion rate.

The distribution of the gas density as a function of y points to a large deviation from the one-dimensional treatment, particularly at the condensation "jump" and directly behind

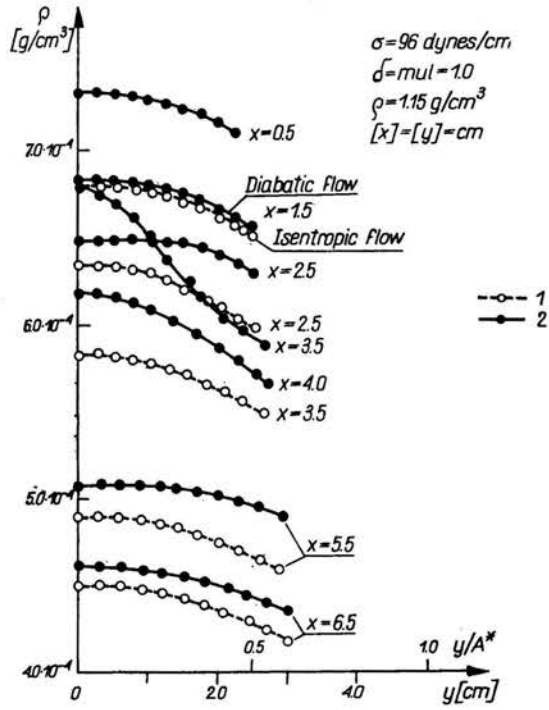

FIG. 11. Gas density as a function of y for various cross-sections of the nozle:
1 — ○ — — isentriopc flow, 2 — ● — diabaric flow,
$\sigma = 96$ dynes/cm, $\varrho_c = 1.15\,\mathrm{g/cm^3}$, $\delta = 1.0$.

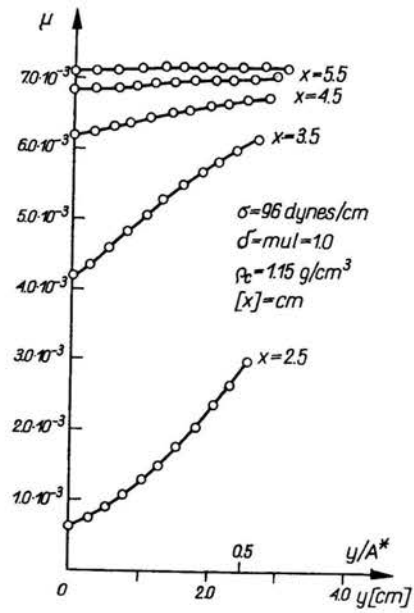

FIG. 12. Solid phase mass fraction as a function of y for various cross-sections of the nozzle:
$\sigma = 96$ dynes/cm, $\varrho_c = 1.15\,\mathrm{g/cm^3}$, $\delta = 1.0$.

it (Fig. 11). Such a deviation between one- and two-dimensional approach is also observed in the case of the distribution of a solid phase mass fraction as a function of y (Fig. 12).

Numerical results for the two-dimensional flow are compared with the experimental ones obtained by M. JAESCHKE at the Göttingen Max Planck Institute [12].

The results of the two-dimensional problem agree better with experiment both at the wall and at the symmetry axis than in the case of one-dimensional flow for various surface tension and correction factors of nucleation rate (Fig. 13).

The one-dimensional treatment changes the qualitative picture of the flow with a phase change at the wall and particularly along axis of symmetry of the nozzle.

The density distribution obtained experimentally differs more from the one-dimensional numerical approximation than from numerical results of the two-dimensional flow. The density distribution (two-dimensional flow) along the nozzle axis has "jump"

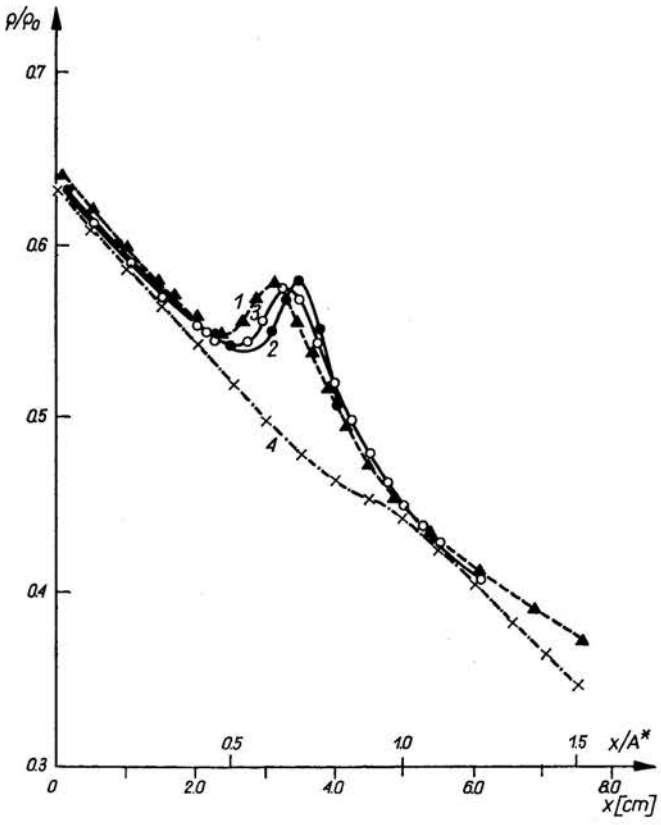

FIG. 13. The comparison of a gas density for two- and one-dimensional flows with experiment (axis of the nozzle):

1 — — ▲ — — experimental results obtained by a pressure measurement, 2 — ● — experimental results from the Mach-Zehnder interferometer, 3 — ○ — two-dimensional flow, 4 —·— × —·— one-dimensional flow, $\varrho_c = 1.15\,\mathrm{g/cm^3}$, $\sigma = 96\,\mathrm{dynes/cm}$, $\delta = 1.0$.

structure, in which we observe the density rise from the point of maximum supercooling to the point of reaching the thermodynamic equilibrium. This has been confirmed by experiment.

The numerical values of the gas density (Fig. 13) are situated between the experimental results obtained: (1) by the pressure measurement along the nozzle axis (curve 1), (2) from interferograms of the Mach-Zehnder interferometer (curve 2).

The pressure distribution for a two-dimensional approach points to a very good agreement with experimental data (Fig. 14).

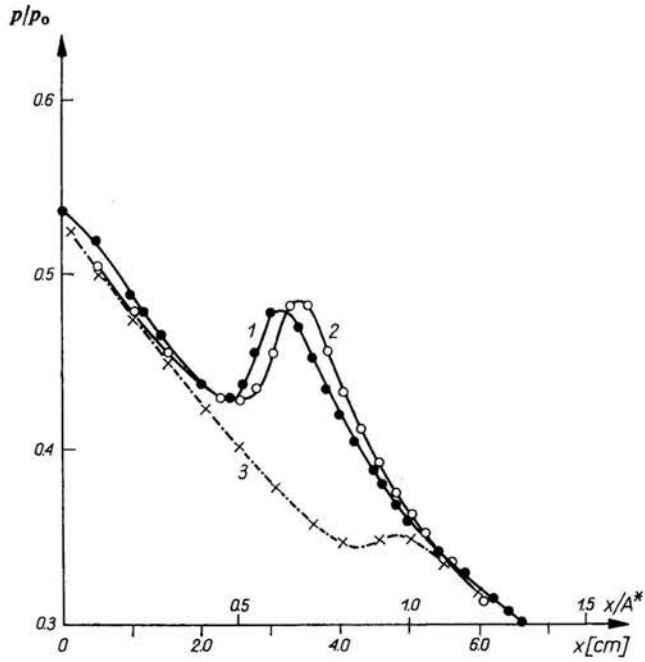

FIG. 14. The comparison of a gas pressure for two- and one-dimensional flows with experiment (axis of the nozzle):
1 — ● — experimental results obtained by the pressure measurement, 2 — ○ — numerical results (two-dimensional flow), 3 —·— × —·— numerical results (one-dimensional flow).

In the one-dimensional treatment, the region of the intensive phase change appears more downstream and the slope of a curve of a pressure distribution is different from the experimental result (along the axis).

5. Conclusions

The following conclusions can be formulated:

1. A two-dimensional approach changes appreciably the qualitative picture of the diabatic flow. It takes place even in the case of de Laval nozzle with small expansion rate. In spite of the fact that in this case the one-dimensional flow approximates well the real two-dimensional isentropic flow, the two-dimensional geometry changes the qualitative picture of the diabatic flow.

2. The above conclusion implies that nozzle geometry influences strongly the character of the flow with the phase change.

3. In the case of the two-dimensional flow, maximum supercooling and the appearance of a condensation zone takes place at a higher pressure and at a lower Mach number.

4. The zone of phase change from the point of maximum supercooling to the point of reaching the thermodynamic equilibrium is narrower in the two-dimensional flow than in the one-dimensional one. Experimental results confirm this point.

5. If a solid phase is formed, the nucleation rate obtained by a semi-empirical approach is the same as for a classical Frenkel, Zeldovich model.

References

1. G. M. POUND, L. A. MADONNA, C. M. SCIULLI, Proc. Conf. Int. Phenomena and Nucleation, Airforce Cambridge Research Center, Geophys. Res. Pap., No. 137, 1955.
2. J. MAYBANK, B. J. MASON, *The production of ice crystals by large adiabatic expansions of water vapour*, Proc. Phys. Soc., **74**. Part I, 475, 11–16, 1959.
3. B. J. MASON, *The physics of clouds*, Oxford Univ. Press, London 1957.
4. P. G. HILL, *Condensation of water vapour during supersonic expansion in nozzles*, J. Fluid Mech., **56**, Part 3, 593–620, 1966.
5. D. BARSCHDORFF, *Verlauf der Zustandsgrössen und gasdynamische Zusammenhänge bei der spontanen Kondensation reinen Wasserdampfes in Lavaldüsen*, Forsch. Ing. Wes., **37**, 5, 146–157, 1971.
6. J. FRENKEL, *Kinetic theory of liquids*, Chap. 7, Oxford University Press, 1946.
7. P. P. WEGENER, J. Y. PARLANGE, *Non-equilibrium nozzle flow with condensation*, AGARD Conf. Proc. No 12, Recent Advances in Aerothermochemistry, ed. I. GLASSMAN, **2**, 12, 607–634, 1967.
8. T. ALTY, C. A. MACKAY, Proc. Roy. Soc. A, **149**, 104, 1935.
9. M. BRATOS, M. BURNAT, *Application of Lax scheme to the computation of transonic flow*, Bull. Acad. Polon. Sci., Série Sci. Techn., **16**, 2, 85–89, 1968.
10. M. BRATOS, M. BURNAT, W. J. PROSNAK, *Application of the Lax finite difference scheme to transonic flow problems*, Fluid Dynamics Transactions, **5**, Part II, 57–65, 1965.
11. D. EUVRARD, J. HUBERT, F. RIGAUT et G. TOURNEMINE, *Calcul numérique d'un écoulement sonique autour d'un profil d'aile d'avion par une méthode inverse*, présentée par M. Paul GERMAIN, C. R. Acad. Sc. Paris, **273**, 739–742, 18 Octobre 1971, Série A.
12. M. JAESCHKE, *Dämpfung von Druck- und Dichteschwankungen in einem schallnahen Freistrahl durch kondensierten Wasserdampf* (Dissertation), Max-Planck-Institut für Strömungsforschung Göttingen 1973.

POLISH ACADEMY OF SCIENCES
INSTITUTE OF FUNDAMENTAL TECHNOLOGICAL RESEARCH.

Received September 13, 1973.